
Wasserstein Distributionally Robust Shallow Convex Neural Networks

Julien Pallage

Department of Electrical Engineering
Polytechnique Montréal, GERAD, & Mila

Antoine Lesage-Landry

Department of Electrical Engineering
Polytechnique Montréal, GERAD, & Mila

Abstract

In this work, we propose Wasserstein distributionally robust shallow convex neural networks (WaDiRo-SCNNs) to provide reliable nonlinear predictions when subject to adverse and corrupted datasets. Our approach is based on a new convex training program for ReLU shallow neural networks which allows us to cast the problem as an exact, tractable reformulation of its order-1 Wasserstein distributionally robust equivalent. Our training procedure is conservative by design, has low stochasticity, is solvable with open-source solvers, and is scalable to large industrial deployments. We provide out-of-sample performance guarantees and show that hard convex physical constraints can be enforced in the training program. WaDiRo-SCNN aims to make neural networks safer for critical applications, such as in the energy sector. Finally, we numerically demonstrate the performance of our model on a synthetic experiment and a real-world power system application, i.e., the prediction of non-residential buildings' hourly energy consumption. The experimental results are convincing and showcase the strengths of the proposed model.

Keywords: distributionally robust optimization, shallow convex neural networks, trustworthy machine learning, physics constrained, energy.

1 Introduction

Neural networks (NNs) have been traditionally overlooked in critical sectors, e.g., energy [1], healthcare [2], and finance [3]. Even though they tend to be successful nonlinear predictors, their lack of interpretability, limited out-of-the-box performance guarantees, complex training procedures, as well as high susceptibility to data corruption and other adversarial attacks, have labelled them as unreliable for such applications. Many solutions have been proposed in the past decade to guide and frame their training as much as possible, e.g., blackbox optimization (BBO) algorithms with provable convergence properties for hyperparameter tuning [4, 5], tight MLOps (contraction of Machine Learning, software development and operations) procedures for lifecycle management [6], post-training verification frameworks [7, 8, 9], introduction of physical knowledge into the models [10, 11], or a combination of them [12]. These methods were pursued to make up for the fact that **(i)** neural networks generally have a non-convex loss function with respect to their weights as well as their hyperparameters [13, 14]; **(ii)** their high complexity and opacity make them unpredictable and theoretical verification is mandatory for complete performance assessment; **(iii)** it is hard to guarantee their out-of-sample performance over time as their drift needs to be monitored; **(iv)** their training often requires a large amount of data and physical insights greatly reduce the data requirements [15]. Nevertheless, these methods contribute to an even higher training complexity and do not scale easily for large deployments.

In this work, we are interested in neural networks with guarantees emerging from the training procedure itself. Our motivation is to develop a scalable nonlinear predictor with inherent theoretical guarantees and low-stochasticity training for large-scale critical applications, e.g., virtual power plants [16], where reliable forecasts of distributed assets are crucial for the safe operation of the electrical power grid.

We specifically target the prediction of the localized impact of non-residential buildings enrolled in demand response programs, e.g., energy consumption or peak-shaving potential. Because of their size and diverse activities, non-residential buildings have complex consumption patterns that require prediction tools able to model such complexity, e.g., neural networks. As each building needs its own model, scalability issues

arise when utilizing complex ML training procedures. Finally, the sensitivity of the application, and the risk associated with poor predictions, promote models with theoretical guarantees and robustness to possible anomalies in the training data, e.g., numerical errors, noise in sensor readings, telemetry issues, meters outage, and unusual extreme events [17].

1.1 Related Work

We now review the bodies of literature closest to ours.

Convex training of neural networks Convex optimization for machine learning (ML) training is desirable as a convex training program guarantees convergence to the minimal loss. In recent years, [18] have shown that training a feedforward shallow neural network (SNN), i.e., a one-hidden layer NN, with ReLU activation functions is equivalent to a convex training procedure. They also extended their results to convolutional neural networks. More importantly, they fundamentally linked ReLU-SNN training problem to a regularized convex program. Following, [19] have obtained an efficient convex training procedure of SNNs with GPU acceleration, and [20] have designed an adversarial training by controlling the worst-case output of the neural network in a neighbourhood around each training samples. In this work, we generalize the regularization procedure of feedforward SNNs in regression tasks through the lens of distributionally robust optimization with the Wasserstein metric.

Distributionally robust neural networks Distributionally robust optimization (DRO), in ML, aims at minimizing the expected training loss of a model over the most adverse data distribution within a distance of the training samples. It minimizes the worst-case out-of-sample risk associated with the training of the model [21]. Different authors have worked on distributionally robust neural networks. Reference [22] have trained deep neural networks using the first-order approximation of the Wasserstein DRO loss function for backpropagation. The authors of [23] have developed a DRO gradient estimator that integrates into neural networks' optimization pipeline similarly to the widely used stochastic gradient descent (SGD) optimizer. In [24], the authors have proposed a method to train deep NNs in a DRO fashion by defining the ambiguity set with groups of the training data and increasing regularization. These methods integrate distributional robustness in the training procedure of deep NNs but do not directly tackle the Wasserstein DRO problem, or an equivalent reformulation. Our proposition, while only applying to shallow networks, works with the tractable reformulation of the Wasserstein DRO problem proposed by [25].

Physics-informed neural networks The training approach for physics-informed neural networks primarily involves a weighted multi-objective function designed to narrow the gap between labels and model predictions while penalizing physical constraints violation. This is achieved by simultaneously minimizing the residuals of a partial differential equation (PDE) and its boundary conditions [15]. The loss terms related to the PDE are derived through the automatic differentiation of the neural network's outputs [26]. This complex loss function is then progressively optimized through backpropagation within the network. While authors of [15] note that boundary conditions can be strictly imposed during training by forcing a part of the network to satisfy these conditions, see [27], they are typically integrated as penalty terms within the loss function. Physics-informed neural networks are characterized by their extensive modelling capabilities, facilitated by automatic differentiation, that allows for the approximation of continuous PDEs across various neural network architectures, e.g., CNNs [28], LSTMs [29], BNNs [30], and GANs [31]. Although limited to convex constraints, in this work, we demonstrate that our training methodology can enforce hard constraints on the shallow network's output during training. These constraints may include, but are not limited to, boundary constraints, ramping constraints, and constraints derived from discrete-time dynamical systems.

Application As stated earlier, prediction algorithms used to forecast non-residential buildings' consumption patterns must respect some inherent constraints. They need to be computationally lightweight, they must be able to model nonlinearities, and the sensibility of the application requires trustworthiness in their predictions, e.g., robustness, interpretability, and guarantees. Because grid operators do not generally have access to information on building activity, occupancy, and control, data-driven approaches tend to be the default option [32]. Authors have used support vector regression (SVR) [33] and other hybrid methods leveraging both classification and linear regression to satisfy the aforementioned constraints [32]. These methods are linear by parts and can approximate nonlinear distributions adequately. Statistical methods such as ARIMA [34] and Gaussian processes have also proved to be good contenders as they offer empirical uncertainty bounds [35]. Many authors have proposed deep-learning methods, yet these propositions do not have much industrial acceptability as they fail to meet the industrial constraints, and thus are not considered. In this work, we show

that our proposition is interesting for virtual power plant applications where the forecast of many distributed assets is used for critical decision-making as we satisfy all industrial constraints better than other comparable models.

1.2 Contributions

We leverage recent results from distributionally robust optimization and convex learning to propose a new Wasserstein distributionally robust shallow convex neural network (WaDiRo-SCNN) with out-of-sample performance guarantees and simple low-stochasticity training. The training is formulated as a convex optimization problem efficiently solvable with open-source solvers. This training problem can be constrained to account for hard physical constraints as long as they are convex. We first benchmark our model with a numerical study in a controlled synthetic environment. We then apply our approach to distribution feeder-specific impact prediction of non-residential buildings enrolled in a demand response program. To the best of our knowledge, our specific contributions are as follows:

- We demonstrate that the SCNN with ℓ_1 -loss training problem is similar to a linear regression over a modified sample space.
- We formulate an exact, tractable, and low-stochasticity Wasserstein distributionally robust training program for shallow convex neural networks under both ℓ_1 -norm and ℓ_2 -norm order-1 Wasserstein distances.
- We derive out-of-sample guarantees for WaDiRo-SCNNs with ℓ_1 -loss training via Rademacher complexity.
- We show that hard convex physical constraints can be easily included in the training procedure of SCNNs with ℓ_1 -norm loss and their WaDiRo counterpart.
- We illustrate the conservatism of WaDiRo-SCNNs in predicting synthetic benchmark functions with controlled data corruption and its performance in predicting real-world non-residential buildings' consumption patterns.

2 Preliminaries

We start by covering the fundamentals of Wasserstein distributionally robust optimization before introducing shallow convex neural networks.

2.1 Distributionally Robust Optimization

Distributionally robust optimization (DRO) minimizes a worst-case expected loss function over an ambiguity set, i.e., an uncertainty set in the space of probability distributions [21]. The problem can be formulated as:

$$\inf_{\beta} \sup_{\mathbb{Q} \in \Xi} \mathbb{E}^{\mathbb{Q}}[h_{\beta}(\mathbf{z})], \quad (\text{DRO})$$

where $\mathbf{z} \in \mathcal{Z} \subseteq \mathbb{R}^d$, $d \in \mathbb{N}$, is a random sample, \mathcal{Z} is the set of all possible values of \mathbf{z} , \mathbb{Q} is a distribution from the ambiguity set Ξ , $\beta \in \mathbb{R}^p$ is the p -dimension decision vector, and $h_{\beta}(\mathbf{z}) : \mathcal{Z} \times \mathbb{R}^p \mapsto \mathbb{R}$ is the loss function when applying β on a sample [25, 36].

We are interested in a data-driven branch of DRO which defines the ambiguity set as a Wasserstein ball centered on an empirical distribution containing N samples: $\hat{\mathbb{P}}_N = \frac{1}{N} \sum_{i=1}^N \delta_{\mathbf{z}_i}(\mathbf{z})$, where $\delta_{\mathbf{z}_i}(\cdot)$ is a Dirac delta function assigning a probability mass of one at each known sample \mathbf{z}_i . Note that as the number of samples goes to infinity the empirical distribution converges to the true distribution \mathbb{P} . The Wasserstein distance, also called optimal transport, can be pictured as the minimal effort that it would take to displace a given pile (d_1) of a weighted resource, e.g., dirt, to shape a second specific pile (d_2). The effort of a trip is given by the distance travelled and the weight of the carried resource. Specifically, it provides a sense of similarity between the two distributions. Formally, the order- t Wasserstein distance between distributions \mathbb{U} and \mathbb{V} is:

$$W_{\|\cdot\|,t}(\mathbb{U}, \mathbb{V}) = \left(\min_{\pi \in \mathcal{P}(\mathcal{Z} \times \mathcal{Z})} \int_{\mathcal{Z} \times \mathcal{Z}} \|\mathbf{z}_1 - \mathbf{z}_2\|^t d\pi(\mathbf{z}_1, \mathbf{z}_2) \right)^{1/t},$$

where \mathbf{z}_1 and \mathbf{z}_2 are the marginals of \mathbb{U} and \mathbb{V} , respectively [36].

In this context, (DRD) is expressed as:

$$\inf_{\beta} \sup_{\mathbb{Q} \in \Omega} \mathbb{E}^{\mathbb{Q}}[h_{\beta}(\mathbf{z})] \quad (\text{WDRO})$$

with $\Omega = \{\mathbb{Q} \in \mathcal{P}(\mathcal{Z}) : W_{\|\cdot\|, t}(\mathbb{Q}, \hat{\mathbb{P}}_N) \leq \epsilon\}$,

where Ω is the order- t Wasserstein sphere of radius $\epsilon > 0$ centered on $\hat{\mathbb{P}}_N$, and $\mathcal{P}(\mathcal{Z})$ is the space of all probability distributions with support on \mathcal{Z} . In a way, ϵ can be interpreted as a hyperparameter that controls our conservatism towards $\hat{\mathbb{P}}_N$. This problem is not tractable [25].

Using the strong duality theorem and the order-1 Wasserstein metric, [25] showed that a tractable reformulation of (WDRO) is obtainable if $h_{\beta}(\mathbf{z})$ is convex in $\mathbf{z} \in \mathcal{Z} = \mathbb{R}^d$, where d is the dimension of the samples. The problem to consider then becomes:

$$\inf_{\beta} \sup_{\mathbb{Q} \in \Omega} \mathbb{E}^{\mathbb{Q}}[h_{\beta}(\mathbf{z})] = \inf_{\beta} \kappa + \frac{1}{N} \sum_{i=1}^N h_{\beta}(\mathbf{z}_i) \quad (\text{TWDRD})$$

s.t. $\kappa = \sup\{\|\boldsymbol{\theta}\|_* : h_{\beta}^*(\boldsymbol{\theta}) < +\infty\}$,

where $\|\cdot\|_*$ is the dual norm $\|\boldsymbol{\theta}\|_* \equiv \sup_{\|\mathbf{z}\| \leq 1} \boldsymbol{\theta}^{\top} \mathbf{z}$ and $h_{\beta}^*(\boldsymbol{\theta})$ is the convex conjugate of $h_{\beta}(\mathbf{z})$, $h_{\beta}^*(\boldsymbol{\theta}) = \sup_{\mathbf{z}} \{\boldsymbol{\theta}^{\top} \mathbf{z} - h_{\beta}(\mathbf{z})\}$ [37].

Training machine learning models with (WDRO) has been proved to be a generalization of regularization [38]. By training over the worst-case expected distribution in a Wasserstein ball centered on the training dataset, we avoid overfitting on the empirical distribution and become more robust against outliers, anomalies, and some adversarial attacks.

2.2 Shallow Convex Neural Networks

Let $\mathbf{X} \in \mathbb{R}^{N \times d}$ be a data matrix of N feature vectors, $\mathbf{x}_i \in \mathbb{R}^d \forall i \in \{1, 2, \dots, N\} \equiv \llbracket N \rrbracket$, and $\mathbf{y} \in \mathbb{R}^N$ be the corresponding one-dimensional labels. Define data samples as a feature-label pair: $\mathbf{z}_i = (\mathbf{x}_i, y_i) \forall i \in \llbracket N \rrbracket$. The non-convex training problem of a single-output feedforward shallow neural network (SNN) with ReLU activation functions is as follows:

$$p^* = \min_{\mathbf{W}_1, \mathbf{w}_2} \mathcal{L} \left(\mathbf{y}, \sum_{i=1}^m \{(\mathbf{X}\mathbf{W}_1)_i + w_{2i}\} \right), \quad (\text{SNNT})$$

where m is the number of hidden neurons, $\mathbf{W}_1 \in \mathbb{R}^{d \times m}$, and $\mathbf{w}_2 \in \mathbb{R}^m$ are the weights of the first and second layers, $\mathcal{L} : \mathbb{R}^N \rightarrow \mathbb{R}$ is a convex loss function, and $(\cdot)_+$ is an element-wise $\max\{0, \cdot\}$ operator.

The convex reformulation of the SNN training problem (SNNT) is based on an enumeration process of all the possible ReLU activation patterns in the hidden layer for a fixed training dataset \mathbf{X} [18]. The enumeration is equivalent to generating all possible hyperplane arrangements passing through the origin and clustering the data with them. The set of all possible activation patterns a ReLU NN can take for a training set \mathbf{X} is given by:

$$\mathcal{D}_{\mathbf{X}} = \{\mathbf{D} = \text{diag}(\mathbb{1}(\mathbf{X}\mathbf{s} \succeq \mathbf{0})) : \mathbf{s} \in \mathbb{R}^d\}, \quad (1)$$

where \mathbf{D} is a diagonal matrix with a possible activation pattern encoded on the diagonal, $\mathbb{1}$ is the indicator function, and \succeq is an element-wise \geq operator.

By introducing cone-constrained variables $\boldsymbol{\nu}, \boldsymbol{\omega} \in \mathbb{R}^{P \times d}$ and the diagonal matrices from $\mathcal{D}_{\mathbf{X}}$, [18] have obtained a convex training procedure from which we can find the previous non-convex weights under some conditions. The optimization problem is now defined as

$$p^* = \min_{\boldsymbol{\nu}, \boldsymbol{\omega}} \mathcal{L} \left(\sum_{D_i \in \mathcal{D}_{\mathbf{X}}} \mathbf{D}_i \mathbf{X}(\boldsymbol{\nu}_i - \boldsymbol{\omega}_i), \mathbf{y} \right) \quad (\text{SCNNT})$$

s.t. $\boldsymbol{\nu}_i, \boldsymbol{\omega}_i \in \mathcal{K}_i \quad \forall i \in \llbracket P \rrbracket$,

where $\mathcal{K}_i = \{\mathbf{u} \in \mathbb{R}^d : (2\mathbf{D}_i - \mathbf{I})\mathbf{X}\mathbf{u} \succeq \mathbf{0}\}$ and $P = \text{card}(\mathcal{D}_{\mathbf{X}})$. For $m \geq m^* = \sum_{i: \boldsymbol{\nu}_i \neq \mathbf{0}} 1 + \sum_{i: \boldsymbol{\omega}_i \neq \mathbf{0}} 1$, problems (SNNT) and (SCNNT) have identical optimal values [18]. The relation between the optimal weights

of each problem is then given by:

$$(\mathbf{W}_{1i}^*, \mathbf{w}_{2i}^*) = \left(\frac{\boldsymbol{\nu}_i^*}{\sqrt{\|\boldsymbol{\nu}_i^*\|_2}}, \sqrt{\|\boldsymbol{\nu}_i^*\|_2} \right), \quad \text{if } \boldsymbol{\nu}_i^* \neq \mathbf{0}, \forall i \in \llbracket P \rrbracket \quad (2)$$

$$(\mathbf{W}_{1(i+P)}^*, \mathbf{w}_{2(i+P)}^*) = \left(\frac{\boldsymbol{\omega}_i^*}{\sqrt{\|\boldsymbol{\omega}_i^*\|_2}}, -\sqrt{\|\boldsymbol{\omega}_i^*\|_2} \right), \quad \text{if } \boldsymbol{\omega}_i^* \neq \mathbf{0}, \forall i \in \llbracket P \rrbracket. \quad (3)$$

To make the problem computationally tractable, we can relax the full hyperplane arrangements by sampling random vectors [19]. For example, using a Gaussian sampling, we substitute $\mathcal{D}_{\mathbf{X}}$ by $\tilde{\mathcal{D}}_{\mathbf{X}} = \{\mathbf{D}_i = \text{diag}(\mathbb{1}(\mathbf{X}\mathbf{S}_i \succeq \mathbf{0})) : \mathbf{S}_i \sim \mathcal{N}_d(\boldsymbol{\mu}, \boldsymbol{\Sigma}), \mathbf{S}_i = \mathbf{s}_i, \mathbf{D}_i \neq \mathbf{D}_{j \neq i}, i \in \llbracket P \rrbracket\}$ where \mathbf{S}_i is a random Gaussian vector of mean $\boldsymbol{\mu} \in \mathbb{R}^d$ and of covariance $\boldsymbol{\Sigma} \in \mathbb{R}^{d \times d}$, and \mathbf{s}_i is the realization of random vector $\mathbf{S}_i \forall i \in \llbracket P \rrbracket$. This relaxation has the same minima as (SCNNT) if

$$m \geq b := \sum_{\mathbf{D}_i \in \tilde{\mathcal{D}}} \{\boldsymbol{\nu}_i^* : \boldsymbol{\nu}_i^* \neq \mathbf{0}\} \cup \{\boldsymbol{\omega}_i^* : \boldsymbol{\omega}_i^* \neq \mathbf{0}\}, \quad (4)$$

where $\boldsymbol{\nu}^*, \boldsymbol{\omega}^*$ are global optima of (SCNNT) and the optimal activations are in the convex model. Interested readers are referred to [18, 19] for the detailed coverage of SCNNs. We remark that if this condition is met, for a feature sample \mathbf{x} not included in the training set \mathbf{X} , then the non-convex formulation of the neural network gives the same output as the convex formulation when using the same set of realized sampling vectors $\mathcal{S} = \{\mathbf{S}_1 = \mathbf{s}_1, \mathbf{S}_2 = \mathbf{s}_2, \dots, \mathbf{S}_P = \mathbf{s}_P\}$. This notion will be useful in the next section.

3 WaDiRo SCNNs

We now introduce WaDiRo-SCNNs and provide tractable procedures to train them. First, we reexpress the training function of the SCNN in a form compatible with the tractable formulation of the Wasserstein DRO problem from [25] to obtain performance guarantees for critical applications.

We make the following assumption on samples from \mathbb{P} .

Assumption 1. *Samples $\mathbf{z} = (\mathbf{x}, y) \in \mathcal{Z} = \mathbb{R}^{d+1}$ are independent and identically distributed (i.i.d.).*

This is a common assumption in statistical machine learning which is also made by, e.g., [25, 36]. Let $d_{ji} = \mathbf{D}_i(j, j)$, $\mathbf{d}_j \in \{0, 1\}^P$. We consider the modified features $\hat{\mathbf{x}}_j^\top = (\text{vec}(\mathbf{x}_j \mathbf{d}_j^\top)^\top, \text{vec}(\mathbf{x}_j \mathbf{d}_j^\top)^\top)^\top \forall j \in \llbracket N \rrbracket$.

Lemma 1. *Suppose that the training loss function \mathcal{L} is the ℓ_1 -norm and let $\hat{\mathbf{z}}_j = (\hat{\mathbf{x}}_j, y_j) \ j \in \llbracket N \rrbracket$ be modified samples. Then, the convex training procedure (SCNNT) is equivalent to a linear regression problem.*

Following Lemmas 1 and 2, we consider the new empirical distribution of the modified samples conditioned on \mathcal{S} : $\hat{\mathbb{F}}_N^{\mathcal{S}} = \frac{1}{N} \sum_{j=1}^N \delta_{\hat{\mathbf{z}}_j | \mathcal{S}}(\hat{\mathbf{z}} | \mathcal{S})$, where $\hat{\mathbf{z}}_j = (\hat{\mathbf{x}}_j, y_j)^\top$. We formulate the non-tractable Wasserstein distributionally robust training problem of the SCNN by centering the Wasserstein ball on $\hat{\mathbb{F}}_N^{\mathcal{S}}$:

$$\begin{aligned} & \inf_{\beta} \sup_{\mathbb{Q} \in \Omega} \mathbb{E}^{\mathbb{Q}}[g_{\beta}(\hat{\mathbf{z}}) | \mathcal{S}] && \text{(WDR-SCNNT)} \\ \text{s.t.} \quad & \boldsymbol{\nu}_i, \boldsymbol{\omega}_i \in \mathcal{K}_i \quad \forall i \in \llbracket P \rrbracket \\ & \Omega = \{\mathbb{Q} \in \mathcal{P}(\hat{\mathcal{Z}}) : W_{\|\cdot\|, t}(\mathbb{Q}, \hat{\mathbb{F}}_N^{\mathcal{S}}) \leq \epsilon\}, \end{aligned}$$

where $\hat{\mathbf{z}} \in \hat{\mathcal{Z}}$ and $\mathcal{P}(\hat{\mathcal{Z}})$ is the space of all possible distributions with support on $\hat{\mathcal{Z}} = \mathbb{R}^{2Pd+1}$.

Proposition 1. *Consider the ℓ_1 -norm training loss function and suppose Assumption 1 holds, then the convex reformulation of (WDR-SCNNT) is given by the following:*

(i) *If the ℓ_1 -norm is used in the definition of the order-1 Wasserstein distance ($W_{\|\cdot\|_{1,1}}$), we have:*

$$\begin{aligned} & \min_{\boldsymbol{\nu}, \boldsymbol{\omega}, a, \mathbf{c}} \quad \epsilon a \quad + \frac{1}{N} \sum_{j=1}^N c_j && \text{(WDR1-SCNNT)} \\ \text{s.t.} \quad & \beta_i \leq a \quad \forall i \in \llbracket 2Pd + 1 \rrbracket \\ & -\beta_i \leq a \quad \forall i \in \llbracket 2Pd + 1 \rrbracket \\ & \boldsymbol{\beta}^\top \hat{\mathbf{z}}_j \leq c_j \quad \forall j \in \llbracket N \rrbracket \\ & -\boldsymbol{\beta}^\top \hat{\mathbf{z}}_j \leq c_j \quad \forall j \in \llbracket N \rrbracket \\ & \boldsymbol{\nu}_i, \boldsymbol{\omega}_i \in \mathcal{K}_i \quad \forall i \in \llbracket P \rrbracket. \end{aligned}$$

(ii) *If the ℓ_2 -norm is used in the definition of the order-1 Wasserstein distance ($W_{\|\cdot\|_{2,1}}$), we obtain:*

$$\begin{aligned} & \min_{\boldsymbol{\nu}, \boldsymbol{\omega}, a, \mathbf{c}} \quad \epsilon a \quad + \frac{1}{N} \sum_{j=1}^N c_j && \text{(WDR2-SCNNT)} \\ \text{s.t.} \quad & \|\boldsymbol{\beta}\|_2^2 \leq a^2 \\ & a \geq 0 \\ & \boldsymbol{\beta}^\top \hat{\mathbf{z}}_j \leq c_j \quad \forall j \in \llbracket N \rrbracket \\ & -\boldsymbol{\beta}^\top \hat{\mathbf{z}}_j \leq c_j \quad \forall j \in \llbracket N \rrbracket \\ & \boldsymbol{\nu}_i, \boldsymbol{\omega}_i \in \mathcal{K}_i \quad \forall i \in \llbracket P \rrbracket. \end{aligned}$$

Proof: Lemma 1 states that the training problem, with respect to the modified samples $\hat{\mathbf{z}}$, is similar to a constrained linear regression. Lemma 2 shows that the distribution of the modified samples is i.i.d. when conditioning on \mathcal{S} . Because (WDR-SCNNT) uses $\hat{\mathbb{F}}_N^{\mathcal{S}}$, by invoking Lemmas 1 and 2, we reformulate (WDR-SCNNT) as a convex program in the form of (TWDR0). The final forms then follows from [25, Theorem 6.3] and [36, Chapter 4]. The detailed proof is provided in Appendix A for completeness. \square

We remark that (WDR1-SCNNT) and (WDR2-SCNNT) can be easily modified to take into account the bias weights of the hidden and output layers of the SNN. The process is as follows: (i) extend \mathbf{X} with a column of ones which is equivalent to adding bias weights in the hidden layer; (ii) let $\boldsymbol{\beta}$ be defined as $(\text{vec}(\boldsymbol{\nu})^\top, \text{vec}(-\boldsymbol{\omega})^\top, b, -1)$ and $\hat{\mathbf{z}}_j$ as $(\text{vec}(\mathbf{x}_j \mathbf{d}_j^\top)^\top, \text{vec}(\mathbf{x}_j \mathbf{d}_j^\top)^\top, 1, y_j)^\top \quad \forall j \in \llbracket N \rrbracket$ where $b \in \mathbb{R}$ is the bias of the sole output neuron. We also remark that both formulations of Proposition 1 are fairly fast to solve with open-source solvers, e.g., Clarabel [39]. By using these formulations to train SNNs, we efficiently obtain an optimal distributionally robust shallow neural network. Recall that the weights from the standard non-convex SNN training problem can be retrieved via (2) and (3).

4 Out-of-sample performance

Next, we establish WaDiRo-SCNN out-of-sample performance. By first computing the Rademacher complexity [40], it is then possible to bound the expected out-of-sample error of our model. We make the following additional assumptions similarly to [36].

Assumption 2. *The norm of modified samples from \mathbb{F}^S are bounded above: $\|\hat{\mathbf{z}}\| \leq R < +\infty$.*

Assumption 3. *The dual norm of the weights is bounded above: $\sup_{\beta} \|\beta\|_* = B_* < +\infty$.*

These assumptions are reasonable as we aim for real-world applications which, by nature, generally satisfy them.

As shown previously, the SCNN training problem is similar to a linear regression. We can follow the procedure used in [36] for linear regressions to bound the performance of WaDiRo-SCNNs.

Proposition 2. *Under Assumptions 1, 2, and 3, and considering an ℓ_1 -loss function, with probability at least $1 - \delta$ with respect to the sampling, the expected out-of-sample error of WaDiRo-SCNNs on $\mathbb{F}^*|\mathcal{S}$ is*

$$\mathbb{E}^{\mathbb{F}^S} [|\beta^{*\top} \hat{\mathbf{z}}| | \mathcal{S}] \leq \frac{1}{N} \sum_{j=1}^N |\beta^{*\top} \hat{\mathbf{z}}_j| + \frac{2B_*R}{\sqrt{N}} + B_*R \sqrt{\frac{8 \ln(2/\delta)}{N}}, \quad (\text{WaDiRo-OSP})$$

for a modified sample $\hat{\mathbf{z}}$ from the true distribution, that was not available for training, where β^* are the optimal weights obtained from (WDR1-SCNNT) or (WDR2-SCNNT).

Moreover, for any $\zeta > \frac{2B_*R}{\sqrt{N}} + B_*R \sqrt{\frac{8 \ln(2/\delta)}{N}}$, we have:

$$\Pr \left(|\beta^{*\top} \hat{\mathbf{z}}| \geq \frac{1}{N} \sum_{j=1}^N |\beta^{*\top} \hat{\mathbf{z}}_j| + \zeta \mid \mathcal{S} \right) \leq \frac{\frac{1}{N} \sum_{j=1}^N |\beta^{*\top} \hat{\mathbf{z}}_j| + \frac{2B_*R}{\sqrt{N}} + B_*R \sqrt{\frac{8 \ln(2/\delta)}{N}}}{\frac{1}{N} \sum_{j=1}^N |\beta^{*\top} \hat{\mathbf{z}}_j| + \zeta}.$$

Proof: By Lemma 1, the WaDiRo-SCNN's training loss function with respect to $\hat{\mathbb{F}}_N^S$ belongs to the following family:

$$\mathcal{H} = \{(\mathbf{x}, y) \mapsto h_{\beta}(\mathbf{x}, y) : h_{\beta}(\mathbf{x}, y) = |y - \mathbf{x}^{\top} \beta|\}.$$

Thus, the bounds follow from [36, Theorem 4.3.3] and [40, Theorem 8]. \square

5 Physical constraints

Compared to traditional physics-informed neural networks [15], as the training problem is a convex program, knowledge of the system can be introduced as hard, convex constraints in the training phase using the decoupled formulation of the SCNN training. Let $\hat{y}_j = (\text{vec}(\boldsymbol{\nu}), \text{vec}(-\boldsymbol{\omega}))^{\top} \hat{\mathbf{x}}_j$, $j \in \llbracket N \rrbracket$. We formulate the physics-constrained SCNN (PCSCNN) training problem as:

$$\begin{aligned} \min_{\boldsymbol{\nu}, \boldsymbol{\omega}} \sum_{j=1}^N |\beta^{\top} \hat{\mathbf{z}}_j| & \quad (\text{PCSCNNT}) \\ \text{s.t. } \hat{y}_j \in \mathcal{Y}_j \quad \forall j \in \llbracket N \rrbracket & \\ \boldsymbol{\nu}_i, \boldsymbol{\omega}_i \in \mathcal{K}_i \quad \forall i \in \llbracket P \rrbracket, & \end{aligned}$$

where $\mathcal{Y}_j \subseteq \mathbb{R}$ is the convex intersection of all physical constraints for sample $j \in \llbracket N \rrbracket$. The constraints are guaranteed to be respected during training, which is generally not the case in common physics-informed NNs. We illustrate some convex constraints with examples:

$$l_j \leq \hat{y}_j \leq u_j \quad \forall j \in \llbracket N \rrbracket \quad (5)$$

$$|\hat{y}_j - \hat{y}_{j-1}| \leq r_j \quad \forall j \in \llbracket N-1 \rrbracket \quad (6)$$

$$\xi_j \leq \sum_{i=1}^j \boldsymbol{\eta}_i^{\top} \mathbf{x}_i + \sum_{i=1}^j \gamma_i \hat{y}_i \leq \bar{\xi}_j \quad \forall j \in \llbracket N \rrbracket \quad (7)$$

where, with respect to sample j and $\forall i \in \llbracket j \rrbracket$, $u_j \in \mathbb{R}$ is an upper bound, $l_j \in \mathbb{R}$ is a lower bound, $r_j \in \mathbb{R}$ is a ramping bound, and (7) is a bounded first-order relation between input and output history with $\xi_j \in$

\mathbb{R} , $\bar{\xi}_j \in \mathbb{R}$, $\boldsymbol{\eta}_i \in \mathbb{R}^d$, $\gamma_i \in \mathbb{R}$, e.g., a discrete-time dynamical equation. We remark that the WaDiRo-SCNN training problem can be similarly modified to consider physical constraints by adding $\hat{y}_j \in \mathcal{Y}_j \forall j \in \llbracket N \rrbracket$ to the constraints of (WDR1-SCNNT) and (WDR2-SCNNT).

6 Numerical study

This section is split into two parts. We first benchmark our approach in a numerical study with data from a controlled environment before showcasing its performance in a real-world power system application.

6.1 Synthetic experiments

6.1.1 Setting

We aim to assess the performance of our model at learning nonlinear functions in heavily corrupted settings, i.e., at being robust against outliers, with a limited amount of training data. To avoid biasing the underlying distribution, we introduce outliers with the sliced Wasserstein distance [41] and a Gaussian noise, in both the training and validation datasets. We choose traditional non-convex benchmark functions: McCormick [42], Picheny-Goldstein-Price (PGP) [43], Keane [44], and Ackley [45]. These functions strike a balance between complexity and tractability. Despite their non-convexity, they exhibit discernable trends and patterns that facilitate learning compared to some other benchmark functions, e.g., Rana or egg-holder [46]. The variation granularity within these functions is moderate ensuring that the learning process is not hindered by excessively fine and extreme fluctuations in the codomain. In a way, this is what we would expect of most real-world regression datasets, e.g., University of California Irvine’s ML repository [47], with the added advantage of being able to control the degree of corruption of the datasets. These functions were generated with the Python library `benchmark` functions [48] and are illustrated in Figure 1.

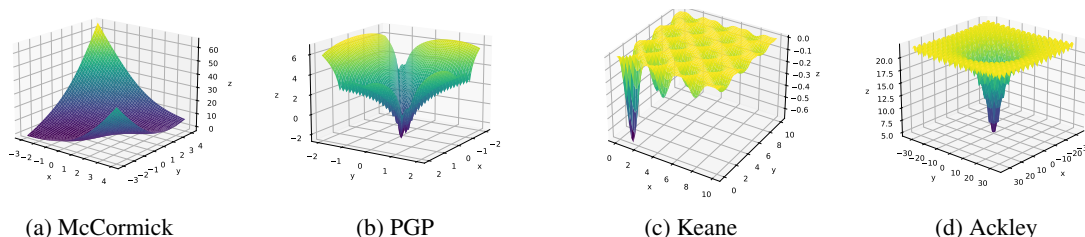


Figure 1: Benchmark functions

We compare our model to an SCNN, a regularized SCNN, a regularized linear regression, a WaDiRo linear regression, and a 4-layer deep ReLU feedforward neural network (FNN) with batch training and dropout layers. Each of these approaches uses a ℓ_1 -loss function. We use simulated annealing [49] for hyperparameter optimization with `hyperopt` [50]. We run 400 trials per ML model, per benchmark function, except for the deep FNN which we limit to 100 trials to mitigate its substantial training time. We split the data such that the training data accounts for 60% of the whole dataset and we split the rest evenly between the validation and the testing phases. We note that the testing data is uncorrupted to measure the ability of each method to learn the true underlying functions without having access to it. We use the mean average error (MAE) for hyperparameter tuning. We also measure the mean squared error (MSE) for additional performance insights. Our whole experiment setup is available on our GitHub page¹ for reproducibility and is delineated in Appendix B. In Experiment A, the outliers are introduced solely in the training data while they are split randomly between training and validation for all the other experiments. Table 1 details the experiment contexts.

¹<https://github.com/jupall/WaDiRo-SCNN>

Table 1: Degree of corruption of each experiment

Experiment	Outlier percentage			Gaussian noise		
	Train.	Val.	Test	Train.	Val.	Test
A	0.4	0	0	True	True	False
B	0.1		0	True	True	False
C	0.4		0	True	True	False

6.1.2 Numerical Results

We now present and analyze the results of each synthetic experiment. Figure 2 shows the normalized error metrics of each model on each function. The normalization is done within each column so that 1.00 and 0.00 represent, respectively, the highest and lowest error between all models for a specific metric and function, e.g., the MAE on McCormick’s function. The absolute values are also presented in Appendix B for additional information.

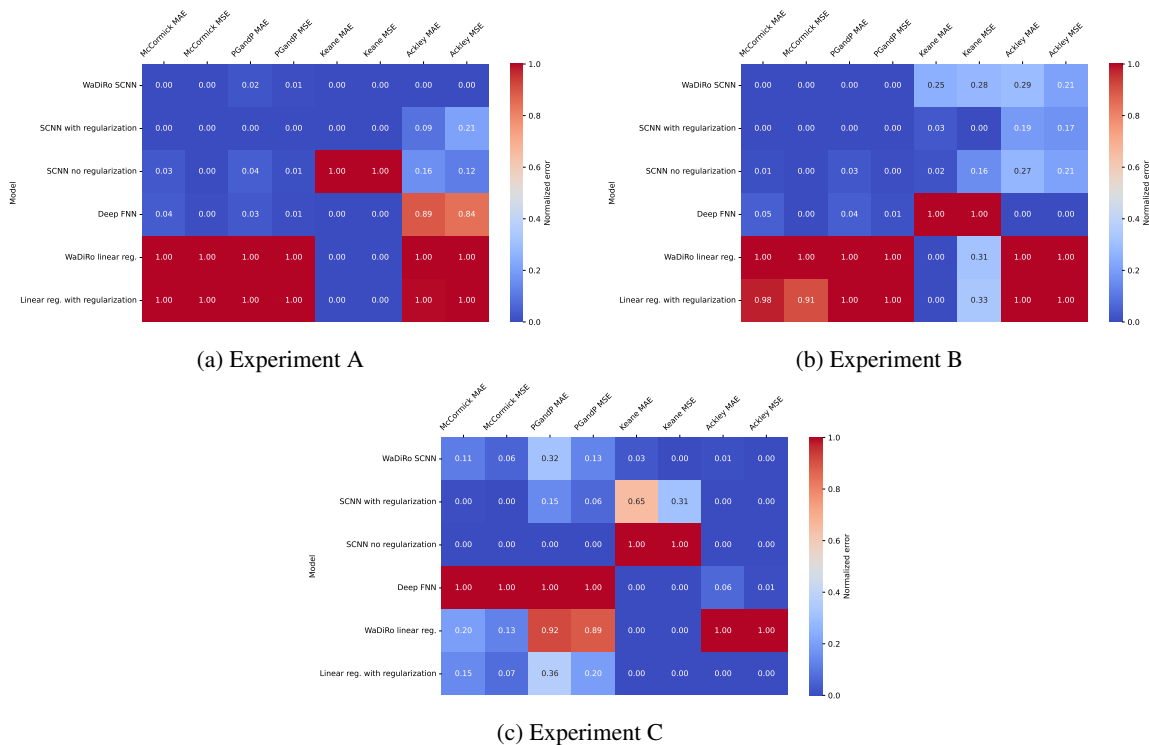


Figure 2: Normalized error of each synthetic experiment

The objective of Experiment A is to evaluate the ability of each model at learning over a highly adversarial training set while having the possibility to refine, indirectly through the validation phase, on a slightly out-of-sample distribution. This experiment was designed to see how different models’ regularization techniques may prevent them from overfitting on training outliers. As we can see, the WaDiRo-SCNN, regularized SCNN, and deep FNN perform similarly except when trying to learn Ackley where the WaDiRo-SCNN has the lowest test error. In this experiment, the linear models perform poorly compared to other models, we hypothesize that the validation phase is uncorrupted enough to let nonlinear models adjust to the non-convex functions during hyperparameter optimization. As expected the non-regularized SCNN leads to performance lower than its regularization counterpart in this particular setting.

In Experiments B and C, outliers are randomly split between training and validation. This implies that models may overfit on outliers during the hyperparameter optimization. Interestingly, in a less corrupted setting, i.e., in Experiment B, we observe that the best models are the nonlinear ones. Yet, when increasing the corruption level, i.e., the ratio of outliers in the data, the linear models become competitive. In both experiments, the

WaDiRo-SCNN’s error is low while not necessarily being the lowest of all models. This is expected as the DRO framework is conservative by definition, maybe even more than other regularization methodologies. This conservatism is what makes it appealing for applications in critical sectors.

We remark that the deep FNN often excels but is subject to its highly stochastic training as there is no guarantee that a good model will be found within the 100 runs made for hyperparameter tuning. Other models, having low-stochasticity training, are easier to tune. We also remark that the non-regularized SCNN performs well but lacks the constancy of its regularized counterparts throughout the experiments.

6.2 Baseline estimation of non-residential buildings

6.2.1 Setting

In 2023, commercial and industrial sectors together represented 49.2% of Québec’s total energy consumption [51]. To accelerate the deployment of Québec’s virtual power plant (VPP), there is need for improving forecasting algorithms for individual non-residential buildings. These algorithms can be used for operations and planning decision-making but also for retroactively calculating rewards associated with shaved energy during demand response events [52]. Non-residential buildings comprise public buildings, e.g., public libraries, schools, and institutional buildings; commercial buildings, e.g., shops, cinemas, and offices; and industrial buildings, e.g., factories and warehouses.

Montréal’s continental humid climate delivers harsh winters and hot summers. As such, a significant amount of energy is consumed for both heating and cooling. Moreover, date and time features have a strong influence on non-residential buildings’ consumption patterns as their activities may change within days and weeks, e.g., opening hours, occupancy, and seasonal activities.

In this experiment, we seek to predict the year-round hourly energy consumption (kWh) of 16 non-residential buildings located in three adjacent distribution substations in Montréal, Québec, Canada. As we do not have any information on building activity, this task is done using only hourly consumption history and historical meteorological features. We use a 12-week history to train each model to predict the following week. We have approximately 2.5 years of collected data on each building. We proceed with a 12-week sliding window and collect the predictions for each new week. We use the data of the first year and a half for hyperparameter tuning and the data of the last year for performance assessment. The features and label are listed in Table 2.

Table 2: Features and label used for the baseline prediction of non-residential buildings

Feature	Name	Domain
1	Day of the week, cosinus encoding	$[0, 1]$
2	Day of the week, sinus encoding	$[0, 1]$
3	Hour of the day, cosinus encoding	$[0, 1]$
4	Hour of the day, sinus encoding	$[0, 1]$
5	Week-end and holiday flag	$\{0, 1\}$
6	Average outside temperature [$^{\circ}\text{C}$]	\mathbb{R}
7	Average solar irradiance [W/m^2]	\mathbb{R}_+
8	Average wind speed [m/s]	\mathbb{R}_+

Label	Name	Domain
1	Hourly energy consumption [kWh]	\mathbb{R}_+

We set cyclical features with a \cos / \sin encoding similarly to [53] and introduce a binary flag to indicate weekends and public holidays. The dataset is created from proprietary data obtained through our collaboration with Hydro-Québec.

To follow the literature, we compare the WaDiRo-SCNN to a Gaussian process (GP), a WaDiRo linear regression, and a linear support vector regression (SVR). We refer readers to Appendix C for details on each model’s hyperparameter search space and the definition of the GP kernel. We limit the hyperparameter tuning to 15 runs per model to represent industrial computational constraints and use the tree-structured parzen esti-

mator (TPE) algorithm proposed by [54] to navigate the search space. We have observed experimentally that TPE converges faster than simulated annealing to good solutions, which suits the limit on runs. The mean average error is used to guide the hyperparameter tuning. We acknowledge that these models are applied naively and that more sophisticated methods could be preferable for this specific real-world application: our goal is to highlight how the WaDiRo-SCNN compares to other models typically used in critical sectors on a real-world dataset and showcase its simplicity. We also test a simple physics-constrained WaDiRo-SCNN in which we enforce that energy consumption must be greater or equal to zero.

6.2.2 Numerical Results

We now proceed with the analysis of our numerical experiments on the prediction of buildings’ consumption patterns. Figure 2 presents the normalized testing errors of each algorithm on each of the 16 tested buildings.

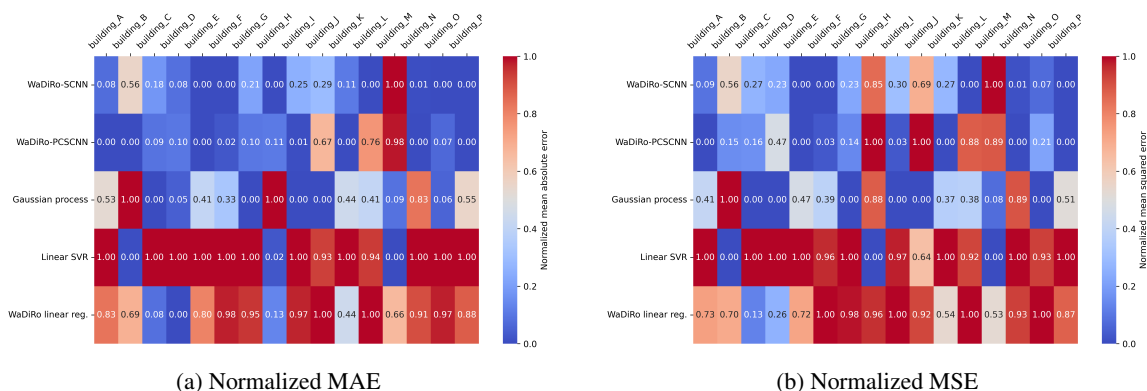


Figure 3: Normalized errors of the hourly baseline prediction of non-residential buildings

Table 3 presents the number of test samples violating the constraint, on non-negative energy consumption, for each model over all buildings and the percentage of deviation from the best model.

Table 3: Number of constraint violations in the testing phase for each model

Model	WaDiRo-PCSCNN	WaDiRo-SCNN	GP	Linear SVR	WaDiRo linear reg.
Violations	1431	2277	2404	4625	3495
Deviation [%]	0.00	59.12	67.99	223.20	144.23

We observe that the WaDiRo-SCNN performs on par with the GP. Still, its performance is slightly above as it has the lower MAE between the two on 10 buildings out of 16 while having similar MSEs. We observe that the linear SVR has the worst performance of all models as it has a consistently lower performance than the WaDiRo linear regression. We observe no significant performance gap between the unconstrained and physics-constrained WaDiRo-SCNNs. We also remark that the physics-constrained WaDiRo-SCNN has the lowest number of constraint violations throughout the experiment. Additional figures, viz., the absolute errors and test prediction plots, are presented in Appendix C for completeness.

We remark that both the GP and our models have different strengths. Our model can include hard physical constraints easily, doesn’t require making assumptions on the type of data seen in training, and is conservative by design. GPs offer empirical uncertainty bounds and can be defined for multiple outputs.

7 Closing remark

In this work, we reformulate the ReLU-SCNN training problem into its order-1 Wasserstein distributionally robust counterpart by using the ℓ_1 -loss function and by conditioning on the set of sampling vectors required by the SCNN. We demonstrate that the training problem has inherent out-of-sample performance guarantees. We show that our settings allow the inclusion of convex physical constraints, which are then guaranteed to

be respected during training. We showcase the conservatism of our model in two experiments: a synthetic experiment with controlled data corruption and the real-world prediction of non-residential buildings' hourly energy consumption.

This work does have some limitations that must be highlighted. The WaDiRo-SCNN training problem is only defined for one output neuron, it is not yet parallelizable and, as most convex optimization problems, it takes an increasing amount of time to solve when augmenting its dimensionality, e.g., the maximal numbers of neurons in the hidden layers, the size of the training set, and the number of features. As such, adapting its formulation for graphics processing unit (GPU) acceleration, similarly to work done by [19], would be interesting. We remark that the integration of physical constraints has not been covered much as it will be investigated further in future works.

Acknowledgments This work was possible thanks to funding from the Fonds de recherche du Québec – Nature et technologies (FRQNT), the Natural Sciences and Engineering Research Council of Canada (NSERC), Mitacs Accelerate, and Hilo by Hydro-Québec. Special thanks to Salma Naccache, Bertrand Scherrer, Steve Boursiquot, Ahmed Abdellatif, and Odile Noël from Hilo.

References

- [1] S. Chatzivasileiadis, A. Venzke, J. Stiasny, and G. Misyris, “Machine Learning in Power Systems: Is It Time to Trust It?” *IEEE Power and Energy Magazine*, vol. 20, no. 3, pp. 32–41, 2022.
- [2] K. Rasheed, A. Qayyum, M. Ghaly, A. Al-Fuqaha, A. Razi, and J. Qadir, “Explainable, trustworthy, and ethical machine learning for healthcare: A survey,” *Computers in Biology and Medicine*, vol. 149, p. 106043, 2022.
- [3] P. Giudici and E. Raffinetti, “SAFE Artificial Intelligence in finance,” *Finance Research Letters*, vol. 56, p. 104088, 2023.
- [4] C. Audet, S. Le Digabel, V. R. Montplaisir, and C. Tribes, “Algorithm 1027: NOMAD Version 4: Nonlinear Optimization with the MADS Algorithm,” *ACM Trans. Math. Softw.*, vol. 48, no. 3, sep 2022.
- [5] K. Kawaguchi and Q. Sun, “A recipe for global convergence guarantee in deep neural networks,” in *Proceedings of the AAAI conference on artificial intelligence*, vol. 35, no. 9, 2021, pp. 8074–8082.
- [6] D. Kreuzberger, N. Kühn, and S. Hirschl, “Machine Learning Operations (MLOps): Overview, Definition, and Architecture,” *IEEE Access*, vol. 11, pp. 31 866–31 879, 2023.
- [7] Y. Huang, H. Zhang, Y. Shi, J. Z. Kolter, and A. Anandkumar, “Training Certifiably Robust Neural Networks with Efficient Local Lipschitz Bounds,” in *Advances in Neural Information Processing Systems*, M. Ranzato, A. Beygelzimer, Y. Dauphin, P. Liang, and J. W. Vaughan, Eds., vol. 34. Curran Associates, Inc., 2021, pp. 22 745–22 757.
- [8] A. Venzke, G. Qu, S. Low, and S. Chatzivasileiadis, “Learning optimal power flow: Worst-case guarantees for neural networks,” in *2020 IEEE International Conference on Communications, Control, and Computing Technologies for Smart Grids (SmartGridComm)*, 2020, pp. 1–7.
- [9] A. Albarghouthi, “Introduction to neural network verification,” *Foundations and Trends® in Programming Languages*, vol. 7, no. 1–2, pp. 1–157, 2021.
- [10] G. E. Karniadakis, I. G. Kevrekidis, L. Lu, P. Perdikaris, S. Wang, and L. Yang, “Physics-informed machine learning,” *Nature Reviews Physics*, vol. 3, no. 6, pp. 422–440, May 2021.
- [11] Y. Xu, S. Kohtz, J. Boakye, P. Gardoni, and P. Wang, “Physics-informed machine learning for reliability and systems safety applications: State of the art and challenges,” *Reliability Engineering & System Safety*, vol. 230, p. 108900, 2023.
- [12] J. Stiasny, S. Chevalier, R. Nellikkath, B. Sævarsson, and S. Chatzivasileiadis, “Closing the loop: A framework for trustworthy machine learning in power systems,” *Proceedings of 11th Bulk Power Systems Dynamics and Control Symposium (IREP 2022)*, 2022.

- [13] I. J. Goodfellow, Y. Bengio, and A. Courville, *Deep Learning*. Cambridge, MA, USA: MIT Press, 2016, <http://www.deeplearningbook.org>.
- [14] J. Sohl-Dickstein, “The boundary of neural network trainability is fractal,” *arXiv preprint arXiv:2402.06184*, 2024.
- [15] S. Cuomo, V. S. Di Cola, F. Giampaolo, G. Rozza, M. Raissi, and F. Piccialli, “Scientific machine learning through physics-informed neural networks: Where we are and what’s next,” *Journal of Scientific Computing*, vol. 92, no. 3, p. 88, 2022.
- [16] D. Pudjianto, C. Ramsay, and G. Strbac, “Virtual power plant and system integration of distributed energy resources,” *IET Renewable power generation*, vol. 1, no. 1, pp. 10–16, 2007.
- [17] L. Zhang, D. Jeong, and S. Lee, “Data Quality Management in the Internet of Things,” *Sensors*, vol. 21, no. 17, 2021.
- [18] M. Pilanci and T. Ergen, “Neural networks are convex regularizers: Exact polynomial-time convex optimization formulations for two-layer networks,” in *International Conference on Machine Learning*. PMLR, 2020, pp. 7695–7705.
- [19] A. Mishkin, A. Sahiner, and M. Pilanci, “Fast Convex Optimization for Two-Layer ReLU Networks: Equivalent Model Classes and Cone Decompositions,” in *International Conference on Machine Learning*, 2022.
- [20] D. Kuelbs, S. Lall, and M. Pilanci, “Adversarial Training of Two-Layer Polynomial and ReLU Activation Networks via Convex Optimization,” *arXiv preprint arXiv:2405.14033*, 2024.
- [21] D. Kuhn, P. M. Esfahani, V. A. Nguyen, and S. Shafieezadeh-Abadeh, “Wasserstein distributionally robust optimization: Theory and applications in machine learning,” in *Operations research & management science in the age of analytics*. Informs, 2019, pp. 130–166.
- [22] X. Bai, G. He, Y. Jiang, and J. Obloj, “Wasserstein distributional robustness of neural networks,” in *Advances in Neural Information Processing Systems*, A. Oh, T. Naumann, A. Globerson, K. Saenko, M. Hardt, and S. Levine, Eds., vol. 36. Curran Associates, Inc., 2023, pp. 26 322–26 347.
- [23] D. Levy, Y. Carmon, J. C. Duchi, and A. Sidford, “Large-Scale Methods for Distributionally Robust Optimization,” in *Advances in Neural Information Processing Systems*, 2020.
- [24] S. Sagawa, P. W. Koh, T. B. Hashimoto, and P. Liang, “Distributionally Robust Neural Networks for Group Shifts: On the Importance of Regularization for Worst-Case Generalization,” 2020.
- [25] P. Mohajerin Esfahani and D. Kuhn, “Data-driven distributionally robust optimization using the Wasserstein metric: Performance guarantees and tractable reformulations,” *Mathematical Programming*, vol. 171, no. 1, pp. 115–166, 2018.
- [26] A. G. Baydin, B. A. Pearlmutter, A. A. Radul, and J. M. Siskind, “Automatic differentiation in machine learning: a survey,” *Journal of Machine Learning Research*, vol. 18, no. 1, p. 5595–5637, jan 2017.
- [27] Q. Zhu, Z. Liu, and J. Yan, “Machine learning for metal additive manufacturing: predicting temperature and melt pool fluid dynamics using physics-informed neural networks,” *Computational Mechanics*, vol. 67, pp. 619–635, 2021.
- [28] H. Gao, L. Sun, and J.-X. Wang, “PhyGeoNet: Physics-informed geometry-adaptive convolutional neural networks for solving parameterized steady-state PDEs on irregular domain,” *Journal of Computational Physics*, vol. 428, p. 110079, 2021.
- [29] R. Zhang, Y. Liu, and H. Sun, “Physics-informed multi-LSTM networks for metamodeling of nonlinear structures,” *Computer Methods in Applied Mechanics and Engineering*, vol. 369, p. 113226, 2020.
- [30] L. Yang, X. Meng, and G. E. Karniadakis, “B-PINNs: Bayesian physics-informed neural networks for forward and inverse PDE problems with noisy data,” *Journal of Computational Physics*, vol. 425, p. 109913, 2021.

- [31] L. Yang, D. Zhang, and G. E. Karniadakis, “Physics-Informed Generative Adversarial Networks for Stochastic Differential Equations,” *SIAM Journal on Scientific Computing*, vol. 42, no. 1, pp. A292–A317, 2020.
- [32] K. Amasyali and N. M. El-Gohary, “A review of data-driven building energy consumption prediction studies,” *Renewable and Sustainable Energy Reviews*, vol. 81, pp. 1192–1205, 2018.
- [33] B. Dong, C. Cao, and S. E. Lee, “Applying support vector machines to predict building energy consumption in tropical region,” *Energy and Buildings*, vol. 37, no. 5, pp. 545–553, 2005.
- [34] G. R. Newsham and B. J. Birt, “Building-level occupancy data to improve ARIMA-based electricity use forecasts,” in *Proceedings of the 2nd ACM Workshop on Embedded Sensing Systems for Energy-Efficiency in Building*, ser. BuildSys ’10. New York, NY, USA: Association for Computing Machinery, 2010, p. 13–18.
- [35] Y. Weng and R. Rajagopal, “Probabilistic baseline estimation via Gaussian process,” in *2015 IEEE Power & Energy Society General Meeting*, 2015, pp. 1–5.
- [36] R. Chen and I. C. Paschalidis, “Distributionally robust learning,” *Foundations and Trends® in Optimization*, vol. 4, no. 1-2, pp. 1–243, 2020.
- [37] S. Boyd and L. Vandenberghe, *Convex optimization*. Cambridge university press, 2004.
- [38] S. Shafieezadeh-Abadeh, D. Kuhn, and P. M. Esfahani, “Regularization via mass transportation,” *Journal of Machine Learning Research*, vol. 20, no. 103, pp. 1–68, 2019.
- [39] P. J. Goulart and Y. Chen, “Clarabel: An interior-point solver for conic programs with quadratic objectives,” Department of Engineering Science, University of Oxford, Tech. Rep., 2024.
- [40] P. L. Bartlett and S. Mendelson, “Rademacher and Gaussian Complexities: Risk Bounds and Structural Results,” in *Journal of Machine Learning Research*, 2003.
- [41] S. Kolouri, K. Nadjahi, U. Simsekli, R. Badeau, and G. Rohde, “Generalized Sliced Wasserstein Distances,” in *Advances in Neural Information Processing Systems*, H. Wallach, H. Larochelle, A. Beygelzimer, F. d’Alché-Buc, E. Fox, and R. Garnett, Eds., vol. 32. Curran Associates, Inc., 2019.
- [42] E. P. Adorio, “MVF - Multivariate Test Functions Library in C for Unconstrained Global Optimization,” Department of Mathematics, U.P. Diliman, Tech. Rep., 2005.
- [43] V. Picheny, T. Wagner, and D. Ginsbourger, “A benchmark of kriging-based infill criteria for noisy optimization,” *Structural and Multidisciplinary Optimization*, vol. 48, 09 2013.
- [44] A. Keane, “Experiences with optimizers in structural design,” in *Proceedings of the conference on adaptive computing in engineering design and control*, vol. 94, 1994, pp. 14–27.
- [45] D. Ackley, *A connectionist machine for genetic hillclimbing*. Springer science & business media, 2012, vol. 28.
- [46] D. Whitley, S. Rana, J. Dzubera, and K. E. Mathias, “Evaluating evolutionary algorithms,” *Artificial intelligence*, vol. 85, no. 1-2, pp. 245–276, 1996.
- [47] M. Kelly, R. Longjohn, and K. Nottingham, “UCI Machine Learning Repository.” [Online]. Available: <http://archive.ics.uci.edu/ml>
- [48] L. Baronti and M. Castellani, “A Python Benchmark Functions Framework for Numerical Optimisation Problems,” School of Computer Science, University of Birmingham, Tech. Rep., 2024.
- [49] L. Ingber, “Simulated annealing: Practice versus theory,” *Mathematical and Computer Modelling*, vol. 18, no. 11, pp. 29–57, 1993.
- [50] J. Bergstra, B. Komer, C. Eliasmith, D. Yamins, and D. D. Cox, “Hyperopt: a python library for model selection and hyperparameter optimization,” *Computational Science & Discovery*, vol. 8, no. 1, p. 014008, 2015.

- [51] J. Whitmore and P.-O. Pineau, “État de l’énergie au québec.” 2024, préparé pour le gouvernement du Québec.
- [52] M. H. Albadi and E. F. El-Saadany, “Demand response in electricity markets: An overview,” in *2007 IEEE Power Engineering Society General Meeting*. IEEE, 2007, pp. 1–5.
- [53] J. Moon, J. Park, E. Hwang, and S. Jun, “Forecasting power consumption for higher educational institutions based on machine learning,” *The Journal of Supercomputing*, vol. 74, pp. 3778–3800, 2018.
- [54] J. Bergstra, R. Bardenet, Y. Bengio, and B. Kégl, “Algorithms for hyper-parameter optimization,” *Advances in neural information processing systems*, vol. 24, 2011.
- [55] S. Diamond and S. Boyd, “CVXPY: A Python-embedded modeling language for convex optimization,” *Journal of Machine Learning Research*, vol. 17, no. 83, pp. 1–5, 2016.
- [56] A. Paszke, S. Gross, F. Massa, A. Lerer, J. Bradbury, G. Chanan, T. Killeen, Z. Lin, N. Gimeshein, L. Antiga, A. Desmaison, A. Kopf, E. Yang, Z. DeVito, M. Raison, A. Tejani, S. Chilamkurthy, B. Steiner, L. Fang, J. Bai, and S. Chintala, “Pytorch: An imperative style, high-performance deep learning library,” in *Advances in Neural Information Processing Systems 32*. Curran Associates, Inc., 2019, pp. 8024–8035.
- [57] F. Pedregosa, G. Varoquaux, A. Gramfort, V. Michel, B. Thirion, O. Grisel, M. Blondel, P. Prettenhofer, R. Weiss, V. Dubourg, J. Vanderplas, A. Passos, D. Cournapeau, M. Brucher, M. Perrot, and E. Duchesnay, “Scikit-learn: Machine learning in Python,” *Journal of Machine Learning Research*, vol. 12, pp. 2825–2830, 2011.

Appendices

A Proof of Proposition 1

Our objective is to rewrite (WDR-SCNNT) in the form of (TWDRO). This proof is derived from results of [36] and is adapted here for completeness. Consider the ℓ_1 -norm loss function, we have $h_\beta(\hat{\mathbf{z}}) = |\hat{\mathbf{z}}^\top \boldsymbol{\beta}|$ and

$$h_\beta^*(\boldsymbol{\theta}) < +\infty \iff \sup_{\hat{\mathbf{z}}: \hat{\mathbf{z}}^\top \boldsymbol{\beta} \geq 0} \{\boldsymbol{\theta}^\top \hat{\mathbf{z}} - \boldsymbol{\beta}^\top \hat{\mathbf{z}}\} < +\infty \text{ and } \sup_{\hat{\mathbf{z}}: \hat{\mathbf{z}}^\top \boldsymbol{\beta} \leq 0} \{\boldsymbol{\theta}^\top \hat{\mathbf{z}} + \boldsymbol{\beta}^\top \hat{\mathbf{z}}\} < +\infty.$$

Considering the two linear optimization problems, we can find the equivalent dual problems A and B with dual variables λ_A, λ_B , respectively.

$$\begin{aligned} \max (\boldsymbol{\theta} - \boldsymbol{\beta})^\top \hat{\mathbf{z}} &\xrightarrow{\text{dual}} \min 0 \cdot \lambda_A && \text{(Dual-A)} \\ \text{s.t. } \hat{\mathbf{z}}^\top \boldsymbol{\beta} &\geq 0 && \text{s.t. } \boldsymbol{\beta} \lambda_A = \boldsymbol{\theta} - \boldsymbol{\beta}, \lambda_A \leq 0, \end{aligned}$$

and

$$\begin{aligned} \max (\boldsymbol{\theta} + \boldsymbol{\beta})^\top \hat{\mathbf{z}} &\xrightarrow{\text{dual}} \min 0 \cdot \lambda_B && \text{(Dual-B)} \\ \text{s.t. } \hat{\mathbf{z}}^\top \boldsymbol{\beta} &\leq 0 && \text{s.t. } \boldsymbol{\beta} \lambda_B = \boldsymbol{\theta} + \boldsymbol{\beta}, \lambda_B \geq 0. \end{aligned}$$

Because the objective function of both dual problems is 0, to have finite optimal values for both primals, (Dual-A) and (Dual-B) need to have a non-empty feasible set.

This implies that these two constraints must be respected:

$$\begin{aligned} \exists \lambda_A \leq 0, \quad \text{s.t. } \boldsymbol{\beta} \lambda_A = \boldsymbol{\theta} - \boldsymbol{\beta} \\ \exists \lambda_B \geq 0, \quad \text{s.t. } \boldsymbol{\beta} \lambda_B = \boldsymbol{\theta} + \boldsymbol{\beta}. \end{aligned}$$

From this we find that

$$|\theta_i| \leq |\beta_i| \quad \forall i, \tag{8}$$

because

$$\begin{aligned} \boldsymbol{\beta}(1 - \lambda_B) &= \boldsymbol{\theta} \text{ with } \lambda_B \geq 0 \\ \boldsymbol{\beta}(1 + \lambda_A) &= \boldsymbol{\theta} \text{ with } \lambda_A \leq 0. \end{aligned}$$

If (8) holds, then both primals are finite. Thus, we have

$$\kappa(\boldsymbol{\beta}) = \sup\{\|\boldsymbol{\theta}\|_* : |\theta_i| \leq \beta_i, \forall i\},$$

and

$$\kappa(\boldsymbol{\beta}) = \|\boldsymbol{\beta}\|_* = \sup_{\|\mathbf{k}\| \leq 1} \boldsymbol{\beta}^\top \mathbf{k}.$$

For the ℓ_1 -loss, when $\|\boldsymbol{\beta}\|_* = \|\boldsymbol{\beta}\|_\infty$, the problem now becomes:

$$\inf_{\boldsymbol{\beta}} \epsilon \|\boldsymbol{\beta}\|_\infty + \frac{1}{N} \sum_{i=1}^N h_{\boldsymbol{\beta}}(\hat{\mathbf{z}}_i). \tag{9}$$

Using the slack variables $a \in \mathbb{R}$ and $\mathbf{c} \in \mathbb{R}^N$ in, respectively, the first and second terms of the objective, yields the equivalent problem:

$$\begin{aligned} \min_{\nu, \omega} \quad & \epsilon a \quad + \frac{1}{N} \sum_{j=1}^N c_j \\ \text{s.t.} \quad & \beta_i \leq a \quad \forall i \in \llbracket 2Pd + 1 \rrbracket \\ & -\beta_i \leq a \quad \forall i \in \llbracket 2Pd + 1 \rrbracket \\ & \beta^\top \hat{\mathbf{z}}_j \leq c_j \quad \forall j \in \llbracket N \rrbracket \\ & -(\beta^\top \hat{\mathbf{z}}_j) \leq c_j \quad \forall j \in \llbracket N \rrbracket \\ & \nu_i, \omega_i \in \mathcal{K}_i \quad \forall i \in \llbracket P \rrbracket. \end{aligned}$$

For the ℓ_2 -loss, $\|\beta\|_*$ is equal to the ℓ_2 -norm [37]. By the same process and noting that $a \geq 0$, because a norm is non-negative, we obtain the second equivalent problem:

$$\begin{aligned} \min_{\nu, \omega} \quad & \epsilon a \quad + \frac{1}{N} \sum_{j=1}^N c_j \\ \text{s.t.} \quad & \|\beta\|_2^2 \leq a^2 \\ & a \geq 0 \\ & \beta^\top \hat{\mathbf{z}}_j \leq c_j \quad \forall j \in \llbracket N \rrbracket \\ & -(\beta^\top \hat{\mathbf{z}}_j) \leq c_j \quad \forall j \in \llbracket N \rrbracket \\ & \nu_i, \omega_i \in \mathcal{K}_i \quad \forall i \in \llbracket P \rrbracket, \end{aligned}$$

which completes the proof. \square

B Complementary materials for the synthetic experiment

In this section, we detail the synthetic experiments of Section 6.1 and we present additional figures.

B.1 Hyperparameters and setting

The hyperparameters of each model are presented in Table 4. Note that all models are formulated with bias weights by default and that different regularization methodologies are cast as hyperparameters in this experiment.

We sample only 2000 data points for each benchmark function before splitting them between training, validation, and training. For the benchmark functions that can be defined in dimension higher than two, viz., Ackley and Keane, we impose a dimension of four.

WaDiRo-SCNNs and SCNNs are modelled and optimized in `cvxpy` [55]. We then extract the weights and encode them into `pytorch`'s neural network module [56]. Similarly, the WaDiRo linear regression and the regularized linear regression are optimized with `cvxpy`, and the deep FNN is fully implemented with `pytorch`.

B.2 Additionnal figures

Figure 4 presents the absolute values of the figures presented in Section 6.1.2.

C Complementary materials for the building experiment

In this section, we detail the experiments on non-residential buildings' baseline prediction from Section 6.2 and we showcase some additional figures of interest.

C.1 Hyperparameters and setting

First, we define the kernel used for the Gaussian process regression. Following our inspection of the data, we construct the GP kernel by adding a radial basis function (RBF) kernel to an exponential sine kernel to

Table 4: Detailed information on the synthetic experiment

Model	Hyperparameter	Description	Possible values
WaDiRo-SCNN	radius	Radius of the Wasserstein ball	$[e^{-8}, e^1]$
	max_neurons	Max number of neurons	$\{10, 11, \dots, 300\}$
	wasserstein	Norm in the order-1 Wasserstein metric	ℓ_1 or ℓ_2
Regularized SCNN	lambda_reg	Regularizing parameter	$[e^{-8}, e^1]$
	max_neurons	Max number of neurons	$\{10, 11, \dots, 300\}$
	regularizer	Regularization framework	Lasso or Ridge
Non-regularized SCNN	max_neurons	Max number of neurons	$\{10, 11, \dots, 300\}$
WaDiRo linear reg.	radius	Radius of the Wasserstein ball	$[e^{-8}, e^1]$
	wasserstein	Norm in the order-1 Wasserstein metric	ℓ_1 or ℓ_2
Regularized linear reg.	lambda_reg regularizer	Regularizing parameter Regularization framework	$[e^{-8}, e^1]$ Lasso or Ridge
Deep FNN	batch_size	Size of each batch	$\{2, 3, \dots, 100\}$
	n_hidden	Number of neurons in hidden layers	$\{10, 11, \dots, 300\}$
	learning_rate	Learning rate	$[e^{-8}, e^1]$
	n_epochs	Number of epochs	$\{2, 3, \dots, 10^3\}$
	dropout_p	Dropout probability at each layer	$[0.01, 0.4]$

model periodicity and a white noise kernel to capture the possible noise. Both the GP and the linear SVR were implemented with `scikit-learn` [57].

Similarly to the previous section, we present, in Table 5, the hyperparameters used in the experiments.

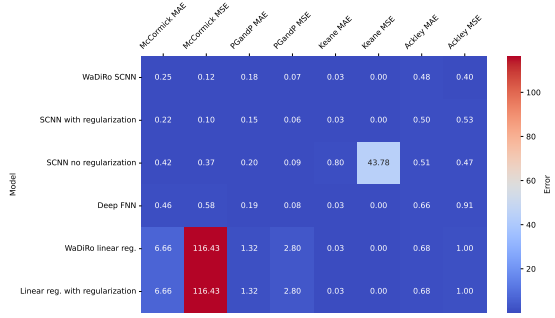
Table 5: Models’ hyperparameters for the building experiment

Model	Hyperparameter	Description	Possible values
WaDiRo-SCNN	radius	Radius of the Wasserstein ball	$[e^{-6}, e^1]$
	max_neurons	Max number of neurons	$\{10, 11, \dots, 70\}$
	wasserstein	Norm in the order-1 Wasserstein metric	ℓ_1 or ℓ_2
WaDiRo linear reg.	radius wasserstein	Radius of the Wasserstein ball Norm in the order-1 Wasserstein metric	$[e^{-6}, e^1]$ ℓ_1 or ℓ_2
Linear SVR	C	Regularizing parameter	$[e^{0.1}, e^7]$
	fit_intercept	Bias	True or False
	loss	Loss function used	ℓ_1 or ℓ_2
Gaussian process	length_scale	Length-scale of the RBF kernel	$[e^{0.1}, e^5]$
	periodicity	Periodicity of the exponential sine kernel	$[e^{0.1}, e^5]$
	length_scale_sine	Length-scale of the exponential sine kernel	$[e^{0.1}, e^5]$
	noise_level	Noise level of the white noise kernel	$[e^{0.001}, e^2]$

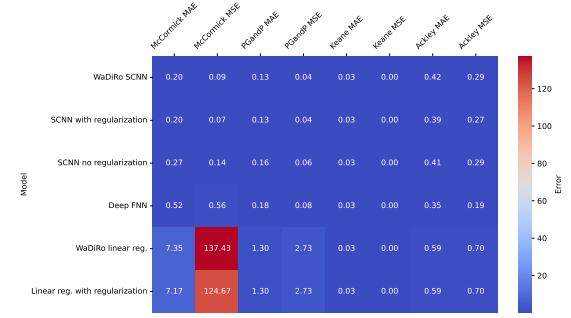
C.2 Additional figures

In Figure 5, we show the absolute values of the errors corresponding to Figure 3.

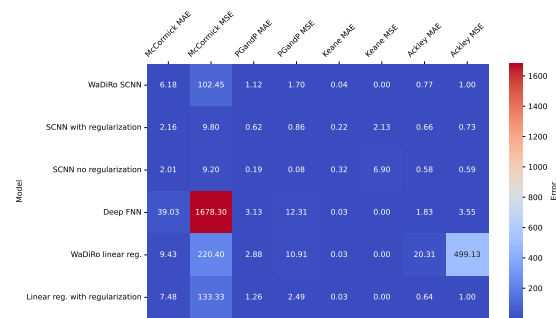
In Figure 6, we present hourly winter predictions from the testing phase. We observe that applying models naively does not always work for every building, e.g., building M.



(a) Experiment A

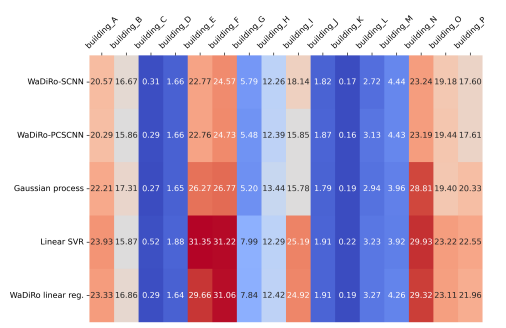


(b) Experiment B

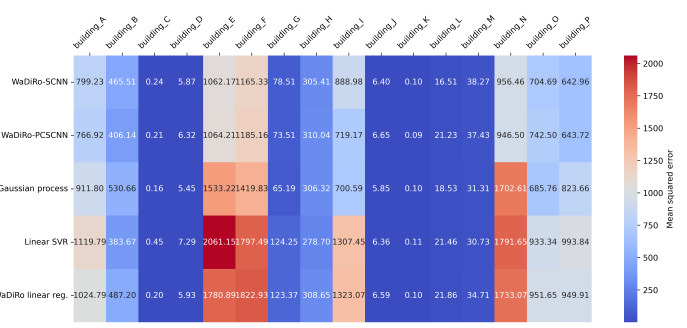


(c) Experiment C

Figure 4: Absolute error of each synthetic experiment



(a) MAE



(b) MSE

Figure 5: Absolute errors of the hourly baseline prediction of non-residential buildings

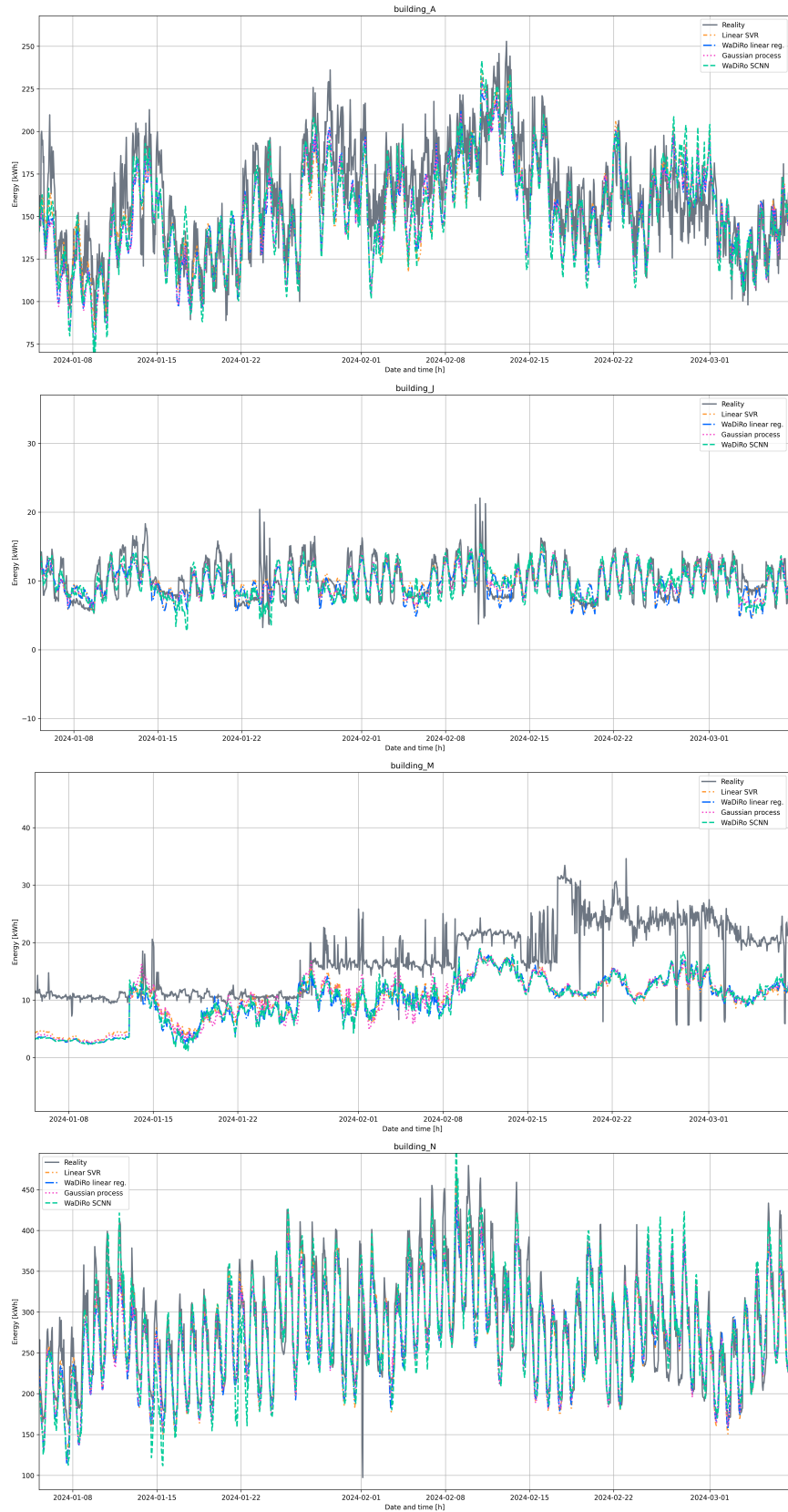


Figure 6: Winter predictions of the testing phase for some buildings